

Thermal Decomposition of Ketene in Shock Waves

Morizo TSUDA*¹ and Kenji KURATANI*Space and Aeronautical Research Institute, The University of Tokyo, Komaba, Meguro-ku, Tokyo*

(Received July 12, 1967)

With the use of a single pulse shock tube of a magic hole type, the thermal decomposition of ketene was studied at temperatures from 1140 to 1530°K. The formation of carbon monoxide, that is, the disappearance of ketene, followed a kinetic order of 1.5 with respect to ketene and its rate constant was represented by

$$k = 10^{14.2} \exp[(-65600 \pm 1100)/RT]^{1/2} \text{ mol}^{-1/2} \text{ sec}^{-1}.$$

The thermal decomposition of mixtures of ketene and ethylene in argon was also studied, and the formation of methylene radicals during the pyrolysis of ketene is deduced from the presence of propylene and cyclo-propane in the products of these three component reactants. The rate of ketene disappearance was not affected by the addition of ethylene, or nitric oxide. A chain mechanism in which methylene radicals play a principal part, and a combined molecular mechanism of first, and second orders were proposed tentatively to explain the observed 1.5th order reaction rate.

Methylene is formed in the thermal decomposition of diazomethane, as well as in the photochemical decomposition of diazomethane and ketene.^{1,2} However, there have been few studies of the thermal decomposition of ketene at high temperatures, and one cannot presume the formation of methylene radicals in the pyrolysis of ketene.

In the rather lower temperature range from 400 to 600°C, Young,^{2,3} and Guenther and Walters⁴ studied the thermal decomposition of ketene and found that the main products in the initial stages were allene and carbon dioxide. On the other hand, data available at higher temperatures are only those of Muller and Peytral,⁴ and they found carbon monoxide and ethylene as the major products at 1150°C. According to these studies, it seems that there is clear difference between the results obtained at different temperatures.

To confirm the formation of methylene radicals in the thermal decomposition of ketene, we have studied the pyrolysis of ketene by the use of a single pulse shock tube. A shock-heating procedure is suitable to generate high temperature, and we were able to investigate the decomposition of ketene in the higher temperature range, and to know whether the mechanism of decomposition at high

temperature is different from that at low temperature or not.

Experimental

Materials. Ketene was prepared according to a modification of Back's method.⁵ Vapor of G. R. grade acetic anhydride in nitrogen carrier gas was heated at 510±5°C in a quartz tube. Unreacted anhydride was removed by passage through a dry ice-acetone trap, and the pyrolyzed products were collected at -196°C. Crude ketene was degassed at -196°C, and purified by repeated distillations at about -120°C (an *n*-propyl alcohol bath was used). Usually purified ketene contains 0.1—0.3% carbon dioxide.*²

One lot of ketene was introduced into a 7 cm long cell at 150 mmHg, and surveyed by an infrared spectrometer. No absorption band was observed except those belonging to ketene. Immediately after purification, ketene was diluted with a large excess of argon to a concentration of 4% or 5%, and the mixture was stored in a 5 l flask at room temperature. At a total pressure of less than 600 mmHg, there was no change in composition during the storage period.

High quality argon, supplied by Tomoe Co. (oxygen content less than 0.2 ppm), and 99.7% ethylene obtained from Takachiho Co. were used without further purification.

Apparatus and Procedure. A single pulse shock tube of a new design, developed at Cornell University,⁶

5) M. H. Back, *Can. J. Chem.* **43**, 106 (1965).

*² One lot of ketene which contained 1.3% carbon dioxide and a trace of ethylene was used to check the effect of impurities, but there was no appreciable effect of carbon dioxide on the reaction rate and product distribution.

6) J. E. Klepeis, Thesis, Graduate School of Aeronautical Eng., Cornell Univ. (1961); A. Lifshitz, S. H. Bauer and E. L. Restler, Jr., *J. Chem. Phys.*, **38**, 2056 (1963). We thank Professor Bauer for his kind advice to construct this tube.

*¹ Present address: Faculty of Hygienical Science, Kitasato University, Shiba-shirogane-sankochō, Minato-ku, Tokyo.

1) H. M. Frey, "Progress in Reaction Kinetics," Vol. 2, Pergamon Press., Oxford (1964), p. 131.

2) J. R. Young, *J. Chem. Soc.*, **1958**, 2909.

3) W. B. Guenther and W. D. Walters, *J. Am. Chem. Soc.*, **81**, 1310 (1959).

4) J. A. Muller and E. Peytral, *Compt. rend.*, **196**, 379 (1933).

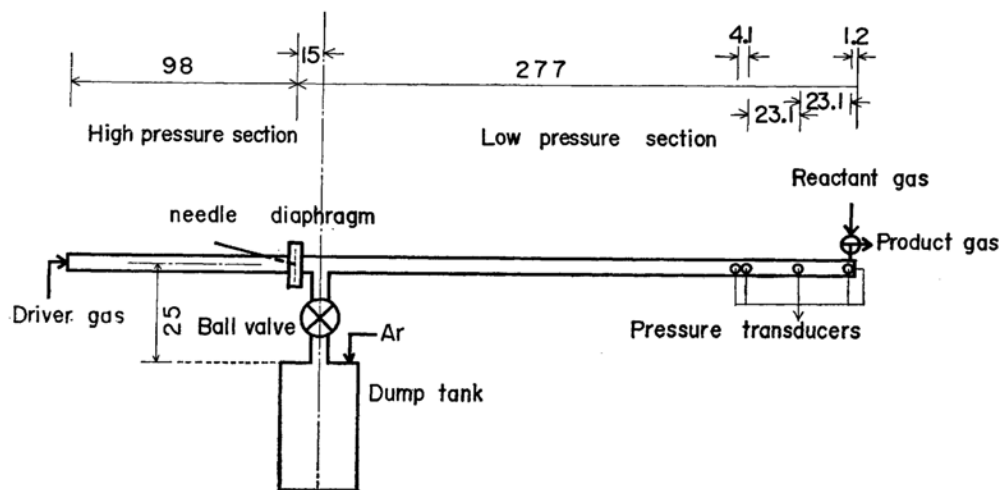


Fig. 1. Single pulse shock tube.

has a dump tank at the upstream end of a driven section. Using this device, it is not necessary to burst out two diaphragms at the preset time interval, and the whole system becomes very simple. We were greatly interested in this new design, and made a tube of this type as shown in Fig. 1. The inner diameter of our tube was 4 cm, and the length of the driver, and the driven sections were 98 and 277 cm, respectively. A dump tank of 19 l volume was attached to the driven section 15 cm downstream from the diaphragm through a branch tube and a ball valve of the same diameter. The main portion of the driven section was made of "Terex" glass, and the driver section of steel tubing, and was equipped with a needle to burst the diaphragms.

Four barium titanate-lead zirconate pressure transducers were mounted on the wall, flush with the inner surface, 51.5, 47.4, 24.3, and 1.2 cm from the end plate. The signals produced by the passage of an incident shock wave over these transducers were fed into amplifiers and converted into pulses by thyatrons. The pulsed output of the first transducer was used to trigger both a raster circuit, and an oscilloscope, to measure the shock velocity, and to show the pressure profile at the downstream end, respectively. Amplified

pulses from the remaining three gauges were recorded on a raster synchroscope system having ten-microsecond marks. The incident shock wave velocity and its mean attenuation at the positions of these gauges were determined by measuring the time interval of the pulses shown on the pictures of the synchroscope display. The observed values of attenuation extended to nearly 0.4% when the incident shock wave travelled the distance of 23.1 cm, and they were taken into account to evaluate the incident shock wave velocity at the downstream end.

One more piezo-electric pressure transducer was embedded in the end plate and was used to measure the pressure profile at the downstream end. The signal from this gauge was displayed on an oscilloscope, and the length of the plateau of the pressure profile was taken as the dwell time of the reaction.

A typical record of this pressure profile is illustrated in Fig. 2.

Prior to an experimental run, both the driver and the driven sections (including the dump tank) were evacuated, the latter especially, attaining a pressure of less than $0.2 \mu\text{Hg}$. Then the valve located between the dump tank and the main driven section was closed, and the former was filled with pure argon, and the latter with the sample gas highly diluted in argon. The pressure of both parts was kept at the same level, and just before pressurization of the driver section, the above valve was again opened.

The sample gas is heated only once by an incident and reflected shock wave in the shock tube. However, the former heating process is ignored, and the temperature behind the reflected shock wave, T_5 , is taken to be the reaction temperature. The temperature T_5 , and the density behind the reflected shock wave were calculated as functions of incident shock wave velocities at the downstream end, assuming that there was no chemical change behind the shock waves. The necessary enthalpy values for ketene at higher temperatures were taken from the table given by Moore and Pimentel,⁷⁾ or calculated using the same

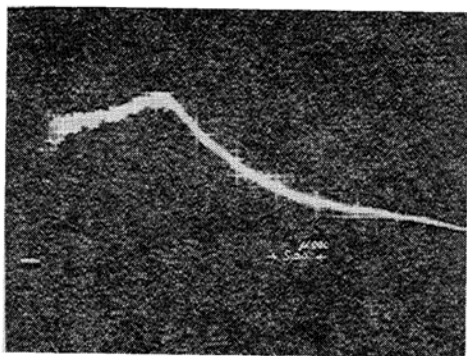


Fig. 2. A typical pressure profile at the end plate. In ordinary cases, pressure behind a reflected shock wave rises gradually, but the slope in Fig. 2 is too high. This disagreement may be derived from the narrowness of our shock tube.

7) C. B. Moore and G. C. Pimentel, *J. Chem. Phys.*, **38**, 2816 (1963).

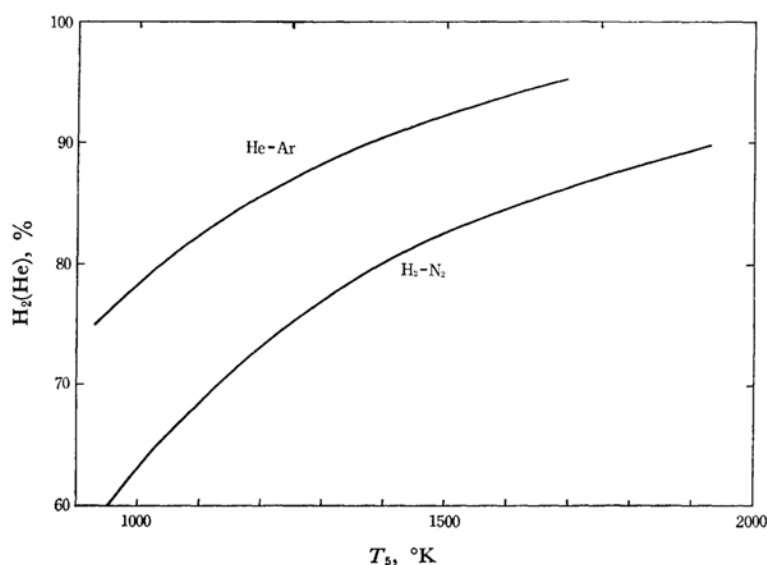
Fig. 3. Optimum composition of driver gas; $T_1=290^\circ\text{K}$, 2.0% ketene in argon.

TABLE I. GAS CHROMATOGRAPHIC ANALYSES

Gas analyzed	Column	Column length	Temp.	Carrier gas	Detector
H ₂ , He	molecular sieve 5A	3 m	room temp.	Ar	catharometer
Ar, N ₂ , CH ₄ , CO	molecular sieve 5A	2 m	100°C	He	catharometer
CH ₄ , CO ₂	charcoal	2 m	100°C	He	catharometer
CH ₄ , C ₂ H ₂	charcoal	2 m	150°C	He	ionizn. flame
C ₂ H ₄ , C ₂ H ₆	7% $\beta\beta'$ -DPN + 93% DBM* in chromosorb + alumina	5 m	room temp.	He	ionizn. flame
C ₃ -hydrocarbons		2 m	150°C		

* H. Miyake and M. Mitooka, *Nippon Kagaku Zasshi* (*J. Chem. Soc. Japan, Pure Chem. Sect.*), **84**, 923 (1963).

molecular parameters adopted by them. To minimize the error in T_3 , caused by neglecting the heat of reaction, most of the kinetic studies were carried out with mixtures of 0.5–2.0% ketene in argon.

"Lumirror" (trade name of poly-ethylene terephthalate, a product of Toyo Rayon Co.) sheets of various thickness were used as diaphragms to separate the higher and lower pressure section. When the pressure and composition of the driver gas were brought to previously determined values, diaphragms were pierced manually with a needle.

To achieve the highest cooling rate with a rarefaction wave, the tube should be tuned so that the head of the wave reflected from the end of the high pressure section, meets the reflected shock wave and the gas interface at approximately the same point. Since the length of the driver section of our tube is fixed at 98 cm, this adjustment was performed by the proper choice of the driver gas composition. A satisfactory composition was obtained according to the shock wave diagram calculation as shown in Fig. 3. Actually, it takes a finite time to rupture the diaphragms, and the calculated composition is regarded as an approximation. Fortunately, however, this estimate was proved to be

accurate enough for our purpose, judging from the pressure profile at the end plate. A mixture of hydrogen and nitrogen was mainly used as the driver gas, and occasionally when it was planned to carry out a complete analysis of the products, a helium-argon mixture was used.

Analytical. The shock heated gas was rapidly cooled by a rarefaction wave, and immediately after the rupture of the diaphragms the reaction mixture was withdrawn to an evacuated vessel of 130 cc volume and analyzed by gas chromatography. A Yanagimoto G. C. G.-3DH gas chromatograph with a flame ionization attachment G. C. F.-103 was used for hydrocarbon analysis. Analyses of inorganic gaseous products were carried out with a usual thermal conductivity cell. In the latter case, in order to raise sensitivity, the output was recorded on a Sanei "Galvanograph", having a sensitivity of 0.25 mV full scale. For the determination of the small amount of hydrogen produced by pyrolysis, a helium-argon mixture was used as the driver gas, since, even if we took extreme care to avoid migration of the driver gas into the sampling vessel, it was almost impossible to keep the reaction products completely free of the driver gas. Therefore, the

contents of the driver gas components were also analyzed for every run, and yields of product gases were corrected in accordance with the amount of driver gas migration.

For the separation of cyclopropane from propylene, a 5 m long column, at room temperature, packed with 7% $\beta\beta'$ -oxy-dipropionitrile and 93% dibutylmaleate on chromosorb was connected in front of an alumina column 2 m in length at 150°C. With the use of this combined column, the relative retention volumes of propane, propylene, acetylene, cyclopropane, and allene to *n*-butane were found to be 0.32, 0.48, 0.56, 0.71, and 0.97, respectively.*³ Columns, and the experimental conditions used by us are shown in Table 1.

Results

On the Products. In several experimental runs we have measured the amount of unreacted ketene through absorption at 2163 and 2135 cm^{-1} , and confirmed that almost all oxygen atoms derived from pyrolyzed ketene are detected as carbon monoxide, and dioxide. This conclusion is consistent with the finding of Young,²⁾ and hereafter we assume that the amount of decomposed ketene is equal to the sum of $[\text{CO}] + 2[\text{CO}_2]$ produced.

TABLE 2. YIELDS OF PRODUCTS IN TYPICAL RUNS

Run No.	Total concn. (ρ_5 in mol/l)	Ketene concn. in %	T_5	Dwell time in ms	Product distributions in %		
					CO	CO ₂	H ₂
577	1.96×10^{-2}	0.5	1530°K	1.40	0.299	0.0043	*
643	3.93×10^{-2}	2.0	1520	1.40	1.19	0.0006	0.170
640	4.01×10^{-2}	2.0	1500	1.40	1.10	0.006	0.156
625	4.11×10^{-2}	2.0	1495	1.30	1.13	0.0077	0.223
642	3.81×10^{-2}	2.0	1475	1.35	1.12	0.0047	0.118
644	3.62×10^{-2}	2.0	1360	1.55	0.619	0.004	0.0177
645	3.57×10^{-2}	2.0	1330	1.55	0.362	0.0011	0.0093
646	3.55×10^{-2}	2.0	1290	1.60	0.154	*	0.0036
674	3.64×10^{-2}	2.0	1260	1.55	0.065	*	0

Run No.	Product distributions in %					
	CH ₄	C ₂ H ₂	C ₂ H ₄	C ₂ H ₆	C ₃ H ₆	C ₃ H ₄
577	0.027	0.037	0.073	0.0072	*	*
643	0.18	0.17	0.12	0.0056	0.0014	0.0023
640	0.15	0.16	0.15	0.010	0.0019	*
625	0.185	0.14	0.13	0.0085	*	*
642	0.17	0.17	0.17	0.010	0.0027	0.0038
644	0.076	0.072	0.12	0.0097	0.0020	0.0038
645	0.041	0.039	0.063	0.0047	0.00097	0.0024
646	0.021	0.017	0.028	0.0017	0.00035	0.0015
674	0.0079	0.0083	0.018	0.00094	*	*

* No analysis was made.

TABLE 3. MASS BALANCES OF PRODUCTS

Run No.	ΣO	ΣC_2	ΣH_2	$\Sigma\text{C}_2/\Sigma\text{O}$	$\Sigma\text{H}_2/\Sigma\text{O}$
643	1.191	0.984	0.960	0.83	0.81
640	1.112	0.951	0.948	0.86	0.85
625	1.146	0.942	1.021	0.82	0.89
642	1.129	1.013	1.028	0.90	0.91
644	0.627	0.562	0.525	0.90	0.84
645	0.364	0.313	0.278	0.86	0.76
646	0.154	0.137	0.128	0.89	0.83
674	0.065	0.064	0.063	0.98	0.97

*³ These values shifted from 0.29, 0.51, 0.77, 0.67, and 1.04 to 0.33, 0.48, 0.50, 0.73, and 0.94 as the alumina column temperature was raised from 120°C

to 170°C. 150°C was the best choice with respect to the separation of acetylene from the other components.

The product distributions of some typical runs are shown in Tables 2 and 3. In these tables, corrected values of $[\text{CO}_2]$, reducing the amounts contained in the original reactant mixtures from the values obtained by the product analyses, are listed, but since the amount of CO_2 in the reactant was comparable to that produced, the values of $[\text{CO}_2]$ shown in these tables are rather erroneous. However, as illustrated in Fig. 4, the ratio of

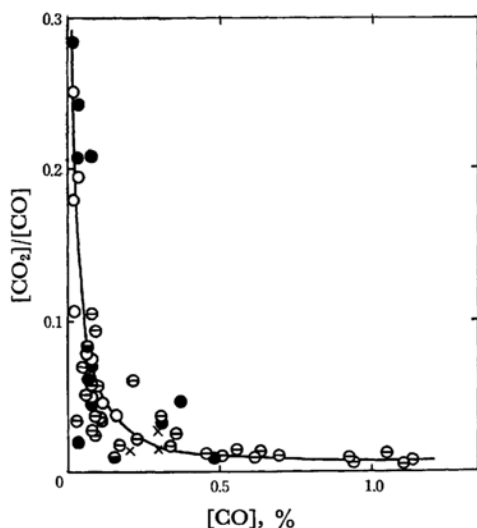


Fig. 4. Relationship between yields of carbon dioxide and carbon monoxide.

× 0.5% mixture ○ 1.0% mixture
 ⊖ 2.0% mixture ● 4.0% mixture
 ● 5.0% mixture

$[\text{CO}_2]/[\text{CO}]$ decreases rapidly with increase in the amount of CO produced. Furthermore, the yield of CO_2 itself is extremely small. Therefore, it seems a good approximation to take the rate of CO formation in place of the pyrolysis rate of ketene itself, especially in the higher temperature range studied by us.

The deficiencies of mass balances of carbon and hydrogen atoms compared with that of the oxygen atom, extend in some cases to 10–20%, and they may be attributable to the formation of a small amount of hydrocarbon polymers and carbon soot. However, when the yields of methane and acetylene are plotted against that of CO , as shown in Fig. 5, linear relationships among the yields of products are revealed, independent of the reaction temperatures and initial concentrations of ketene. That is, the ratios $[\text{CH}_4]/[\text{CO}]$, and $[\text{C}_2\text{H}_2]/[\text{CO}]$ are almost constant and equal to 0.15, and 0.13, respectively, throughout the experimental runs. As for ethylene, the ratio $[\text{C}_2\text{H}_4]/[\text{CO}]$ is held constant at 0.28 as long as the extent of reaction is less than 10%, but when the reaction proceeds further, this ratio decreases gradually.*4 Yields of hydrogen, ethane, and C_3 -

hydrocarbons are relatively small and considered to be minor products.

On the Rate Constant. According to the aforementioned assumption, the initial rate of the thermal decomposition of ketene is transformed to the following equation,

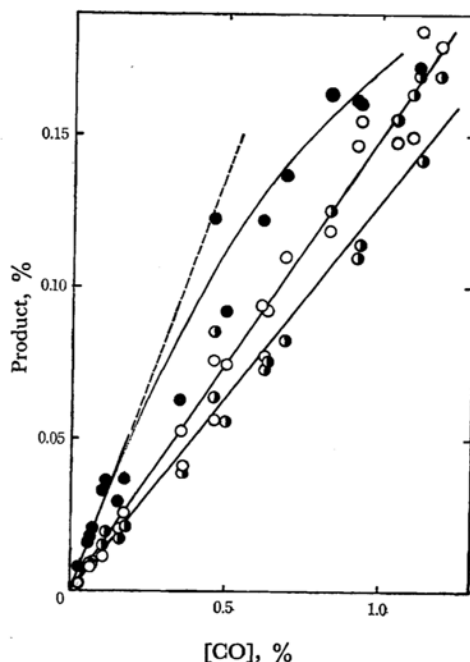


Fig. 5. Yields of methane, acetylene and ethylene.
 ○ methane ⊖ acetylene ● ethylene

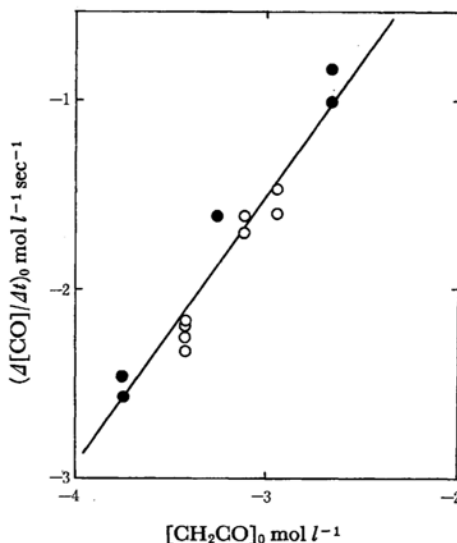


Fig. 6. Determination of reaction order at 1290°K.

*4 Contrary to the formation of ethylene, only small amounts of hydrogen are formed at the lower levels of reaction, but the ratio $[\text{H}_2]/[\text{CO}]$ increases rapidly at higher levels of reaction.

$$(-d[\text{ketene}]/dt)_0 = (d[\text{CO}]/dt)_0 = \Delta[\text{CO}]/\Delta\tau \quad (1)$$

where $\Delta\tau$ represents the dwell time measured at the downstream end. Succeeding this, we assume that the reaction rate is expressed by the formula,

$$\Delta[\text{CO}]/\Delta\tau = k[\text{ketene}]^n[\text{argon}]^m \quad (2)$$

where exponents n and m represent the order with respect to each reactant component.

However, to determine the reaction orders with respect to the initial concentrations of the reactants from Eq. (2), it is necessary to keep the extent of reaction less than 10%, and a reaction temperature of 1290°K was adopted for this reason. The observed rates at 1290°K with the various compositions of ketene and the total pressures are plotted in Fig. 6.

At first, assuming argon to be ineffective, Eq. (2) becomes

$$\Delta[\text{CO}]/\Delta\tau = k'[\text{ketene}]_0^n \quad (3)$$

According to formula (3), the exponent n was determined as the slope of Fig. 6 by a least squares method and found to be

$$n = 1.46 \pm 0.04.$$

In Fig. 6, open circles show the rates obtained with reaction mixtures of the same initial composition. Therefore, in these runs the following relations will hold,

$$[\text{ketene}]_0 \propto [\text{argon}]_0 \propto [\text{total concentration}]_0,$$

and

$$\text{rate} \propto [\text{total concentration}]_0^{n+m}.$$

When attention is paid to only these runs, the abscissa in Fig. 6 can be read as showing total concentrations in arbitrary units. That is, the slope obtained from these experimental points must show the exponent $n+m$. Thus, the total order of the reaction was calculated in a similar manner as

$$n + m = 1.64 \pm 0.08$$

Although the value of $n+m$ is slightly different from that of n , the total order of the reaction is regarded as the same as the order with respect to ketene, and a value of 1.5 was adopted. This conclusion derives the zeroth order with respect to argon, and the assumption made at the beginning may be appreciated.

From the integral formula in the case of a three-halves order reaction, the rate constant is expressed as

$$k = 2\{(C_0/C)^{1/2} - 1\}/C_0^{1/2} \cdot \Delta\tau, \quad (4)$$

where $C_0 = [\text{ketene}]_0$, and $C = [\text{ketene}]_t = C_0 - \Delta[\text{CO}]$. Rate constants at different temperatures from 1140° to 1530°K were calculated by means of Eq. (4) and plotted against the reciprocal of the reaction temperatures. From the Arrhenius plot

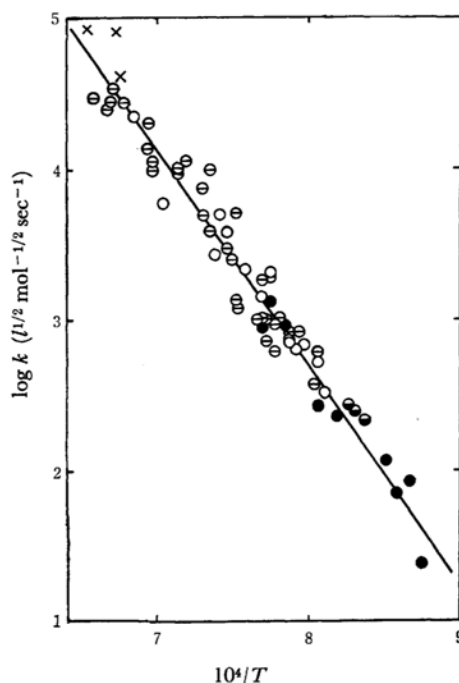


Fig. 7. Arrhenius plot of reaction rate.

× 0.5% ○ 1.0% ⊖ 2.0% ⊖ 4.0% ● 5.0%

in Fig. 7, the apparent activation energy was evaluated as 65.6—1.1 kcal/mol, and finally the rate constant was given by

$$k = 10^{14.15} \exp \{(-65600 \pm 1100)/RT\} \\ l^{1/2} \text{ mol}^{-1/2} \text{ sec}^{-1}$$

Discussion

In the thermal decomposition of ketene at higher temperatures above 1140°K, a small amount of carbon dioxide is found in the final products. For example, when 50% ketene was decomposed, the relative conversion of ketene into carbon dioxide, $2[\text{CO}_2]/([\text{CO}] + 2[\text{CO}_2])$, is only about 1.6%. This fact is in remarkable contrast with the results obtained at temperatures below 900°K, where the relative conversion into carbon dioxide exceeds 50% at the corresponding extent of reaction. Accordingly, we might tentatively ignore the formation of carbon dioxide in the following discussion.

The product distributions of photo-decomposition of ketene at room temperature, which have been studied by Knox⁸⁾ and Chanmugan⁹⁾, are similar to our results. Since it has been established that methylene is an important radical in the photolysis of ketene, the similarity of the product

8) K. Knox, R. G. W. Norrish and G. Porter, *J. Chem. Soc.*, **1952**, 1477.

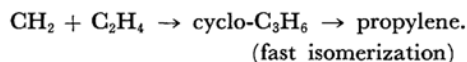
9) J. Chanmugan and M. Burton, *J. Am. Chem. Soc.*, **78**, 509 (1956).

TABLE 4. YIELDS OF C₃-HYDROCARBONS

Run No.	Reaction mixture, in %			Total concn. (ρ_5 in mol/l)	$T_5^\circ\text{K}$	Dwell time msec	Product distributions in % $\times 10^4$			
	ketene	ethylene	argon				C ₃ H ₈	C ₃ H ₆	cyclo-C ₃ H ₆	C ₃ H ₄
651	4.0	4.3	91.7	0.049	1299	1.25	0.6	120	0.7	39
648	4.0	4.3	91.7	0.048	1276	1.20	0.4	80	1.2	35
650	4.0	4.3	91.7	0.043	1132	1.55	0	3	1.0	3.3
652	0	4.0	96.0	0.044	1310	1.40	4	12	0	3
646	2.0	0	98.0	0.036	1290	1.60	0	3	0	15

distributions between the thermal- and photo-decomposition of ketene suggests a resemblance of both reaction schemes. These facts may be interpreted as circumstantial evidence of the formation of methylene radical by the pyrolysis of ketene.

To prove the existence of methylene radicals, the thermal decomposition of ketene containing considerable amounts of ethylene was studied, and a small but not ignorable amount of propylene and a trace of cyclopropane were detected as shown in Table 4. The existence of these molecules in pyrolyzed products supports our aforementioned interpretation, since cyclopropane and propylene may be produced by the reactions



We found another important result from these experiments. That is, the addition of ethylene or NO to ketene scarcely alters the rate of carbon monoxide production.⁵ The rate constants of these mixtures calculated with the 1.5th order rate equation are plotted in Fig. 8 and these rate constants coincide with those obtained from a ketene-argon mixture.⁶ This result excludes a chain reaction mechanism in which a mono-radical plays a main role, and suggests the dominance of a molecular reaction scheme, or the contribution of a bi-radical to the ketene pyrolysis.

We assume further that the small amounts of hydrogen and higher hydrocarbons are obtained as secondary products, and propose the following reaction schemes for the early stage of the thermal decomposition of ketene.

The first of these schemes assumes the following chain reaction mechanism,



⁵ No inhibition of NO to ketene photolysis was already pointed out by Burton *et al.* M. Burton, T. W. Davis, A. Gordon and H. A. Taylor, *J. Am. Chem. Soc.*, **63**, 1956 (1941).

⁶ In fact, the presence of NO rather accelerates the rate of ketene decomposition, as shown in Fig. 8.

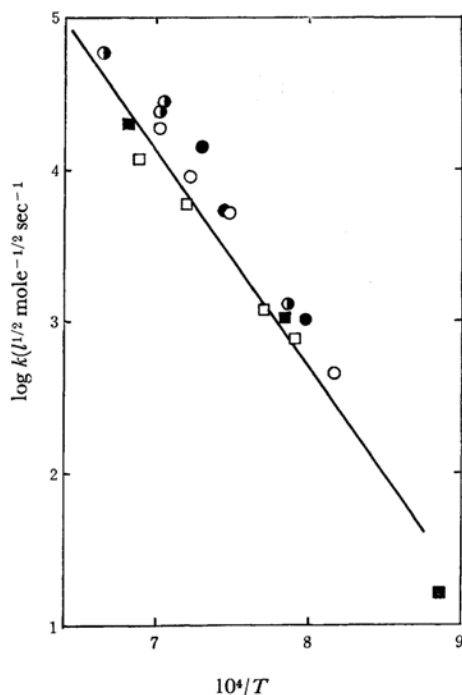
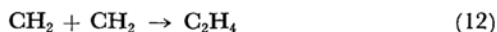
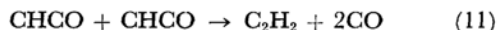
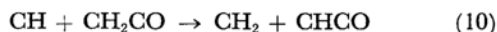


Fig. 8. Effect of ethylene and nitric oxide on the decomposition rate.

- 2% ethylene + 4% ketene
- 4% ethylene + 4% ketene
- 0.2% nitric oxide + 2.0% ketene
- 0.4% nitric oxide + 2.0% ketene



In this scheme, we omit the reaction path to ethane,⁷ since the yield of this substance is very small. Then, the rate of carbon monoxide formation or the thermal decomposition rate of ketene will be expressed as

$$\begin{aligned} -R(\text{ketene}) &= R_5 + R_6 + R_7 + R_8 + R_{10} \\ &= R_5 + R_6 + R_9 + 2R_{11} \end{aligned} \quad (13)$$

⁷ Ethane will be obtained by $\text{CH}_3 + \text{CH}_3 \rightarrow \text{C}_2\text{H}_6$.

where R denotes the rate of an individual step. If one assumes steady state concentrations of radicals, the following relations will be obtained:

$$R_9 = R_{10},$$

$$R_5 + R_{10} = R_6 + R_7 + 2R_{12},$$

$$R_7 = R_8,$$

$$R_7 + R_8 + R_{10} = R_9 + 2R_{11}$$

The second of these equations is rewritten as

$$[\text{CH}_2] = \{-(k_6 + k_7 - k_{10}) + [(k_6 + k_7 - k_{10})^2 + 8k_5k_{12}/[\text{K}]]^{1/2}[\text{K}]\}/4k_{12}$$

where $[\text{K}]$ denotes the concentration of ketene, and if we assume $(k_6 + k_7 - k_{10})^2 [\text{K}]^2$ is very small compared with $8k_5k_{12}[\text{K}]$,^{*8} it follows that

$$[\text{CH}_2] = (k_5[\text{K}]/2k_{12})^{1/2} \quad (14)$$

and the reaction rate is represented by

$$-R(\text{ketene}) = R_5 + 2R_6 + 3R_7 \\ = \{k_5 + 2k_6[\text{K}]^{1/2} + 3k_7[\text{K}]^{1/2}\}[\text{K}]. \quad (15)$$

This expression is consistent with the observed order of the reaction if we ignore the first term. In a similar way, the ratios of methane, acetylene, and ethylene yields against that of CO are given by

$$[\text{CH}_4]/[\text{CO}] = R_7/(2R_6 + 3R_7),$$

$$[\text{C}_2\text{H}_2]/[\text{CO}] = R_7/(2R_6 + 3R_7),$$

$$[\text{C}_2\text{H}_4]/[\text{CO}] = R_6/(2R_6 + 3R_7).$$

Since the yield of ethylene at the lower extent of conversion was about twice as large as that of methane, as shown in Fig. 5, one might assume

$$R_6 = 2R_7,$$

and one can obtain numerical values for these ratios:

$$[\text{CH}_4]/[\text{CO}] = 0.14,$$

$$[\text{C}_2\text{H}_2]/[\text{CO}] = 0.14,$$

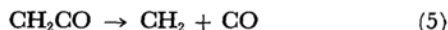
and

$$[\text{C}_2\text{H}_4]/[\text{CO}] = 0.28.$$

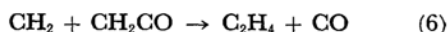
^{*8} In order to derive an expression consistent with the observed order of our reaction rate, this assumption is very useful as shown in the text. But it seems rather artificial and the scheme proposed here should be regarded as a tentative one.

These results are also in excellent agreement with our observations.

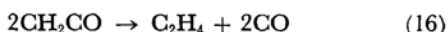
The second proposal assumes the simultaneous decomposition of ketene by first and second order reactions, that is, the first order reactions



and



are combined with the second order reaction



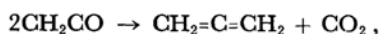
With this tentative frame work, the rate of the carbon monoxide formation will be represented as

$$d[\text{CO}]/dt = k[\text{ketene}]^{1-2}.$$

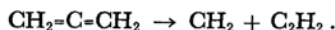
The other products, such as methane and acetylene, will be derived through processes (7)–(11). This scheme is also in agreement with the observed relative yields of methane and acetylene, because

$$[\text{CH}_4]/[\text{C}_2\text{H}_2] = R_8/R_{11} = 2R_8/(R_7 + R_8) = 1.$$

Although experimental results concerning the yield of CO_2 are rather unreliable as already indicated in previous sections, the reaction rate of CO_2 formation in our experiment was found to be roughly proportional to the square of the initial ketene concentration. Moreover, a small amount of allene was detected in the products. These findings are in accord with the reaction path,



proposed by Young,²⁾ and Guenther and Walters.³⁾ Young suggested that allene splits into methylene and acetylene,



This step might be a secondary source of methylene radicals in addition to step (5).

At any rate, in our reaction scheme, methylene radicals may be formed, but it is not certain whether they play a leading role in the reaction sequence or not. The presence of methyl radicals is also demonstrated by the formation of a small amount of ethane as shown in Tables 2 and 3.

The authors wish to thank Messrs. Takuji Sakai and Shiro Hasumi for their assistance in construction of a single pulse shock tube.